International Research Journal on Advanced Engineering and Management
https://goldncloudpublications.com
https://doi.org/10.47392/IRJAEM.2026.0351
e ISSN: 2584-2854
Volume: 04 Issue: 06
June 2026
Page No: 2434 - 2443

# Impact of Renewable Integration with Energy Storage on Grid Stability

*Pranali Pramod Naik[1], Mr. Rupesh Pawaskar[2], Dr. Shridhar S. Khule[3], Mr. Somnath S. Hadpe[4]*
*[1]PG- Electrical Engineering, Matoshri College of Engineering and Research Centre,Nashik,PUNE University, India*
*[2,4]Associate Professor - Electrical Engineering, Matoshri College of Engineering and Research Centre, Nashik, India*
*[3] Head and Professor - Electrical Engineering, Matoshri College of Engineering and Research Centre, Nashik, India*
***Emails:*** *pranalinaik@matoshri.edu.in[1], rupesh.pawaskar@matoshri.edu.in[2], shridhar.khule@matoshri.edu.in[3], somnath.hadpe@matoshri.edu.in[4]*

## Abstract
*The rapid growth of renewable energy integration has introduced new operational challenges in modern power systems due to the variability and uncertainty of sources such as solar and wind. This study examines the influence of renewable penetration on grid stability and investigates the effectiveness of Energy Storage Systems (ESS) in mitigating these impacts.A detailed MATLAB/Simulink model of the IEEE 9-bus system is developed to analyze system behavior under different operating scenarios. Key performance indicators such as voltage profile, frequency stability, and power flow are evaluated with and without ESS integration.Simulation results indicate that ESS significantly enhances system performance by stabilizing voltage levels, improving frequency response, and reducing power fluctuations. The study highlights the importance of coordinated renewable-energy storage integration for reliable and sustainable grid operation.*
***Keywords:*** *Renewable Energy, Energy Storage System, Grid Stability, MATLAB/Simulink, Power System Analysis*

## 1. Introduction
The global shift toward sustainable energy has accelerated the deployment of renewable energy sources in power systems. Technologies such as solar photovoltaic (PV) and wind energy are increasingly being adopted due to their environmental benefits and availability. However, the variability and unpredictability of these sources introduce operational challenges that impact grid stability. Traditional power systems rely on synchronous generators, which naturally provide inertia and support frequency and voltage regulation. With the increasing penetration of inverter-based renewable sources, system inertia is reduced, making the grid more sensitive to disturbances such as sudden load variations and faults. Energy Storage Systems (ESS) have emerged as an effective solution to address these challenges. By storing excess energy during periods of high generation and supplying it during demand, ESS helps maintain system balance and improves reliability. In addition, simulation tools such as MATLAB/Simulink provide a flexible environment for analyzing the behavior of renewable-integrated systems [1-5]. This paper focuses on evaluating the impact of renewable energy integration on grid stability and demonstrates the effectiveness of ESS using the IEEE 9-bus system model.

## 2. Literature Review
Literature Review Comparison Table

**Table 1 Summary of Literature Review**

International Research Journal on Advanced Engineering and Management
https://goldncloudpublications.com
https://doi.org/10.47392/IRJAEM.2026.0351
e ISSN: 2584-2854
Volume: 04 Issue: 06
June 2026
Page No: 2434 - 2443

| Ref. No. | Author(s) | Year | Methodology | Key Contribution | Limitations |
|---|---|---|---|---|---|
| [6] | Y. Zhang et al. | 2020 | Stability analysis of RES | Identified frequency instability issues with high RES penetration | Limited ESS integration study |
| [7] | Molina-García et al. | 2021 | Stochastic optimization | Addressed uncertainty in renewable generation | High computational complexity |
| [8] | X. Luo et al. | 2015 | ESS technology review | Comprehensive study of storage technologies | Lacks real-time application |
| [9] | Bevrani et al. | 2019 | Frequency control using ESS | Improved frequency stability using ESS | Focused on small systems |
| [10] | Teleke et al. | 2020 | Battery control strategies | Effective control of BESS for grid support | Limited hybrid systems |
| [11] | Yang et al. | 2007 | Optimal sizing | Improved efficiency of hybrid RES systems | Old model, lacks modern grid context |
| [12] | Guerrero et al. | 2011 | Microgrid control | Introduced hierarchical control strategies | Not focused on large grids |
| [13] | Shahidehpour et al. | 2021 | Smart grid control | Advanced grid control using AI techniques | Requires high computational resources |

International Research Journal on Advanced Engineering and Management
https://goldncloudpublications.com
https://doi.org/10.47392/IRJAEM.2026.0351
e ISSN: 2584-2854
Volume: 04 Issue: 06
June 2026
Page No: 2434 - 2443

| | | | | | |
|---|---|---|---|---|---|
| [14] | MathWorks | 2024 | MATLAB simulation | Provides simulation framework for RES + ESS | No real hardware validation |

## 3. 3.System Design and Modeling

### 3.1. Photovoltaic (PV) and Energy Storage System (ESS) Integration and Voltage Stabilty.

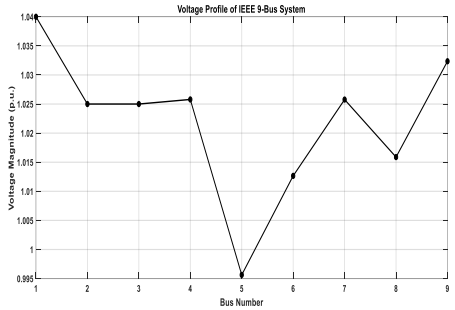


**Figure 1 Voltage Distribution (pu) for IEEE 9-Bus System**

#### 3.1.1. Loss sensitivity factor (LSF) method:

Optimal locations for DG placement are identified using the Loss Sensitivity Factor (LSF) method based on node losses and their sensitivity after compensation [6-10]. The same approach is used to determine suitable locations for EV charging stations. Real and reactive power losses are calculated for all buses, and buses with lower losses and higher strength are selected as the best locations for compensation. Loss sensitivity represents the change in system losses due to compensation provided at a bus. LSF helps reduce the search space by identifying the most suitable candidate buses for placement. Consider a transmission line with impedance (R+jX) connected between buses i and j as shownin Fig 2.

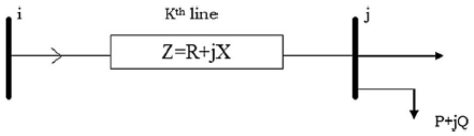


**Figure 2 A Line Section with Connected Load**

Real power loss in the kth line considered in Fig. 1 is given by [Ik2] × [Rk] and can also be expressed as follows,

$$P_{L(j)} = \frac{P^2(j) + Q^2(j) \times R_K}{V(j)^2}$$

Similarly reactive power loss in the kth line is given by [Ik2] × [Xk] and can also be expressed as follows,

$$Q_{L(j)} = \frac{P^2(j) + Q^2(j) \times X_K}{V(j)^2}$$

Where,

- Ik is the current flowing through kth line
- Rk and Xk are the resistance and reactance of the kth line;
- V(j) is the voltage at the bus j
- P(j) = Net Active power supplied beyond the bus j
- Q(j) = Net Reactive power supplied beyond the bus j.

$$LSF = \frac{\partial P_L}{\partial P(j)} = \frac{2 \times P(j) \times R_K}{V(j)^2}$$

$$LSF_1 = \frac{\partial P_L}{\partial Q(j)} = \frac{2 \times Q(j) \times R_K}{V(j)^2}$$

In addition to the MATLAB/Simulink model of the IEEE 9-bus system, a separate MATLAB script was developed to perform Newton–Raphson load flow analysis for detailed system evaluation. The developed code calculated bus voltage magnitudes, voltage angles, and real and reactive power losses under steady-state operating conditions. Furthermore, Loss Sensitivity Factors (LSFs) and the Voltage Stability Index (VSI) were computed to identify the most suitable bus for the integration of

International Research Journal on Advanced Engineering and Management
https://goldncloudpublications.com
https://doi.org/10.47392/IRJAEM.2026.0351
e ISSN: 2584-2854
Volume: 04 Issue: 06
June 2026
Page No: 2434 - 2443

the solar PV plant and Energy Storage System (ESS). The numerical results were presented in tabular form, while voltage profile, LSF, and VSI characteristics were illustrated graphically using plots and bar charts for better system analysis and visualization. The LSF and VSI values were zero for several buses because the adopted formulation depends on the active and reactive power demand connected at each bus. In the IEEE 9-bus system, only buses 5, 6, and 8 contain load demand, whereas the remaining buses mainly operate as generator or transmission buses without local loads, resulting in zero sensitivity values. Higher LSFP and LSFQ values indicate buses that have greater influence on system losses and are therefore more suitable for compensation and distributed generation placement, while lower values indicate comparatively less impact on power loss reduction. Similarly, higher VSI values represent weaker buses that are more prone to voltage instability and collapse, whereas lower VSI values indicate better voltage stability characteristics. The obtained results were presented in Table 2 and graphically represented in Fig. 2 for improved visualization and analysis of overall system performance.

**Table 2 Bus Voltage Profile, Loss Sensitivity Factors (LSFP and LSFQ), and Voltage Stability Index (VSI) of the IEEE 9-Bus System**

| Bus | Vpu | Angle (Deg) | LSFP | LSFQ | VSI |
|---|---|---|---|---|---|
| 1 | 1.04 | 0 | 0 | 0 | 0 |
| 2 | 1.025 | 9.28 | 0 | 0 | 0 |
| 3 | 1.025 | 4.665 | 0 | 0 | 0 |
| 4 | 1.0258 | -2.217 | 0 | 0 | 0 |
| 5 | 0.9956 | -3.989 | 0.02522 | 0.01009 | 0.1715 |
| 6 | 1.0127 | -3.687 | 0.02984 | 0.00995 | 0.10766 |
| 7 | 1.0258 | 3.72 | 0 | 0 | 0 |
| 8 | 1.0159 | 0.728 | 0.01647 | 0.00577 | 0.09767 |
| 9 | 1.0324 | 1.967 | 0 | 0 | 0 |

Top weak buses based on VSI: 5, 6, 8
Top sensitive buses based on LSF: 6, 5, 8

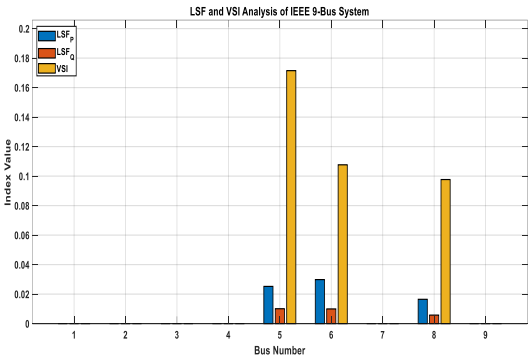


**Figure 2 LSFs and VSI for Load Buses of an IEEE 9-Bus System**

Bus 5 was selected as the optimal location for the integration of the solar photovoltaic (PV) plant and Energy Storage System (ESS) based on Voltage Stability Index (VSI), Loss Sensitivity Factor (LSF), and power flow analysis of the IEEE 9-bus system, as it was identified as the weakest bus. Among all load buses, Bus 5 showed the highest VSI and significant active power loss sensitivity, indicating that power injection at this bus can effectively reduce transmission losses and improve power flow distribution. Its comparatively lower voltage magnitude and higher sensitivity to compensation further confirmed its suitability for renewable energy integration. The coordinated integration of the PV plant and ESS at Bus 5 provides effective active power support to the network. The PV system reduces the loading on conventional generators by supplying local active power, while the ESS compensates for renewable intermittency, improves voltage regulation, enhances transient stability, and supports frequency control during disturbances. In addition, Bus 5 is electrically well connected to the major transmission corridors, enabling efficient distribution of injected power to nearby load buses. The total active load demand of the IEEE 9-bus system is approximately 315 MW. Therefore, the PV plant capacity was selected as 50 MW, corresponding to nearly 15% of the total system demand, which is sufficient to evaluate the impact of renewable integration without causing operational instability. Similarly, the ESS capacity was selected as 50 MWh,

International Research Journal on Advanced Engineering and Management
https://goldncloudpublications.com
https://doi.org/10.47392/IRJAEM.2026.0351
e ISSN: 2584-2854
Volume: 04 Issue: 06
June 2026
Page No: 2434 - 2443

providing adequate energy support for smoothing PV fluctuations, improving voltage stability, supporting fault ride-through capability, and maintaining frequency regulation under dynamic operating conditions.

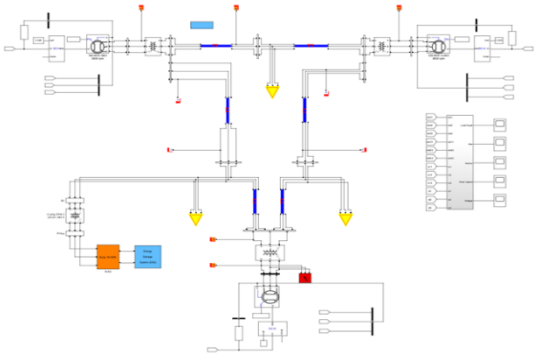

**Figure 3 MATLAB/Simulink Model of an IEEE 9-Bus with PV and ESS System at Bus 5.**

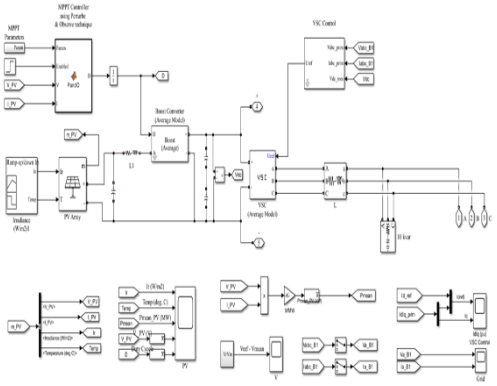

**Figure 4 MATLAB/Simulink Model of the 50 MW Grid-Connected Solar PV System with MPPT and VSC Control**

Fig. 4 shows the MATLAB/Simulink model of the proposed 50 MW grid-connected solar photovoltaic (PV) system integrated through a boost converter and Voltage Source Converter (VSC). The PV array operates under standard test conditions of 1 kW/m² irradiance and 25°C temperature, producing nearly 50 MW output power. A Perturb and Observe (P&O) based Maximum Power Point Tracking (MPPT) controller is used to extract maximum available power from the PV array. The boost converter regulates the DC-link voltage before feeding the VSC, while the VSC synchronizes the PV system with the utility grid and controls active and reactive power injection [11-15]. Measurement blocks monitor PV voltage, current, irradiance, converter output, and grid-side parameters for dynamic performance analysis of the integrated solar power system.

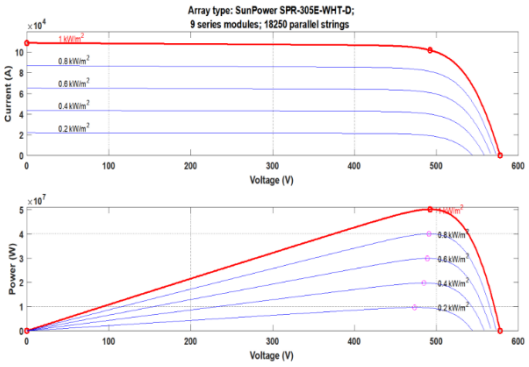


**Figure 5 I-V and P-V Characteristics of the Solar PV Array Under Different Irradiance Levels**

Fig. 5 shows the I–V and P–V characteristics of the SunPower SPR-305E-WHT-D solar PV array consisting of 9 series-connected modules and 18,250 parallel strings under irradiance levels ranging from 0.2 kW/m² to 1 kW/m². The I–V curve shows that the output current increases almost proportionally with irradiance, while the open-circuit voltage remains nearly constant at about 570–580 V. The P–V curve indicates that the maximum output power increases with irradiance, reaching 50 MW at 1 kW/m² and reducing to approximately 40 MW, 30 MW, and 20 MW at lower irradiance levels. The maximum power point (MPP) for all cases occurs within the voltage range of 480–500 V, indicating relatively stable PV voltage with varying output current and power.

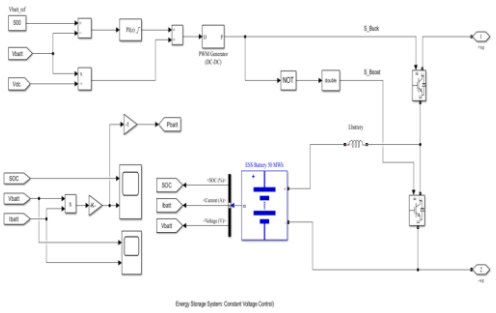

**Figure 6 MATLAB/Simulink Model of the 50 MWh Battery Energy Storage System with Bidirectional DC–DC Converter**

International Research Journal on Advanced Engineering and Management
https://goldncloudpublications.com
https://doi.org/10.47392/IRJAEM.2026.0351
e ISSN: 2584-2854
Volume: 04 Issue: 06
June 2026
Page No: 2434 - 2443

The Fig. 6 illustrates the MATLAB/Simulink model of the 50 MWh Battery Energy Storage System (BESS) integrated with a bidirectional DC–DC converter for constant voltage control. The battery is initialized at 70% state of charge (SOC) to provide sufficient energy for voltage support and dynamic compensation. A PI controller regulates the battery voltage and manages charging and discharging operations through buck and boost modes. The model also monitors SOC, battery voltage, current, and power to evaluate the dynamic performance of the ESS during system operation shown in Table 1-4.

**Table 3 Voltage Profile Comparison of IEEE 9-Bus System.**

| Bus | Voltage (p.u.) | | |
|---|---|---|---|
| | Base Case | Solar+ ESS 50 MW | Solar +ESS 100 MW |
| 1 | 1.0400 | 1.0400 | 1.0400 |
| 2 | 1.0250 | 1.0250 | 1.0250 |
| 3 | 1.0250 | 1.0250 | 1.0250 |
| 4 | 1.0257 | 1.0262 | 1.0248 |
| 5 | 0.9956 | 1.0009 | 1.0037 |
| 6 | 1.0126 | 1.0126 | 1.0110 |
| 7 | 1.0257 | 1.0269 | 1.0274 |
| 8 | 1.0158 | 1.0166 | 1.0166 |
| 9 | 1.0323 | 1.0326 | 1.0323 |

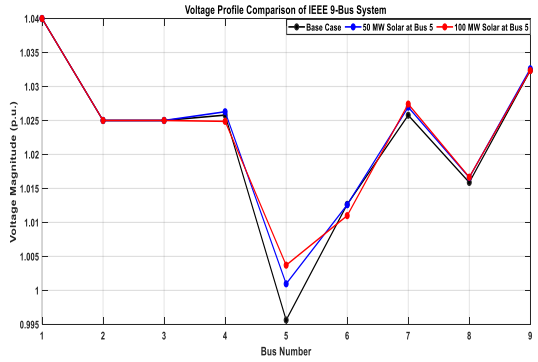


**Figure 7 Voltage Profile Comparison with PV and ESS Connected in System**

The integration of a 50 MW solar photovoltaic (PV) plant and a 50 MWh Energy Storage System (ESS) at Bus 5 was found to effectively improve the voltage stability of the IEEE 9-bus system. Bus 5 was identified as the weakest bus based on voltage profile and stability analysis. The PV system provides local active power support, reducing transmission line loading and improving bus voltage magnitude, while the ESS compensates for PV intermittency and provides fast dynamic support during disturbances. The selected 50 MW PV and 50 MWh ESS capacities were sufficient to enhance voltage regulation and transient stability while maintaining stable system operation. The voltage at Bus 5 improved from 0.9956 p.u. in the base case to 1.0009 p.u. after PV–ESS integration, confirming satisfactory voltage stability enhancement. Although increasing the PV and ESS capacity to 100 MW further improved the voltage to 1.0037 p.u., the additional improvement was very small and caused slight voltage reduction at some buses such as Bus 4 and Bus 6. Moreover, the higher capacity would increase system cost, converter rating, storage requirement, and control complexity without significant technical benefit. Therefore, the 50 MW PV and 50 MWh ESS configuration was identified as the most suitable and economical solution for improving the voltage stability of the IEEE 9-bus system shown in Figure 1-27.

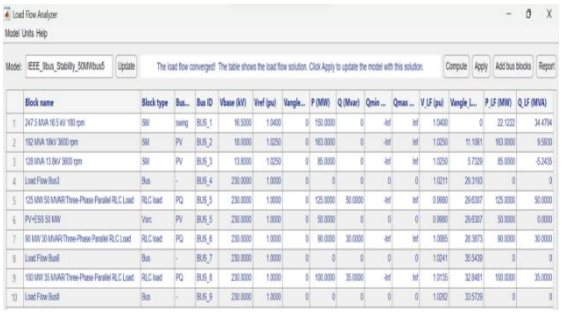

**Figure 8 MATLAB Load Flow Analyzer Results with PV and ESS Connected in System.**

A line outage contingency was simulated by removing the transmission line between Bus 5 and Bus 7 in the IEEE 9-bus system to evaluate voltage stability under disturbed conditions. The outage caused a significant voltage drop at nearby load buses due to interruption of power transfer through the affected transmission corridor. Without the solar PV and ESS system, the voltage at Bus 5 decreased to 0.9380 p.u., which is below the acceptable limit of 0.95 p.u., indicating poor voltage stability. After integrating the 50 MW solar PV plant and ESS at Bus

International Research Journal on Advanced Engineering and Management
https://goldncloudpublications.com
https://doi.org/10.47392/IRJAEM.2026.0351
e ISSN: 2584-2854
Volume: 04 Issue: 06
June 2026
Page No: 2434 - 2443

5, the voltage at Bus 5 improved to 0.9545 p.u., while Bus 7 maintained 1.0173 p.u. The results confirm that the integrated PV and ESS system provides effective active power support and voltage regulation during contingency conditions, while maintaining bus voltages within the acceptable operating range of 0.95–1.05 p.u.

**Table 4 Voltage Profile During Line 5-7 outage for IEEE 9-Bus System**

| Bus | Bus Voltage (pu) | |
|---|---|---|
| | Line Outage | Line Outage + 50 MW PV+ESS |
| 1 | 1.0400 | 1.0400 |
| 2 | 1.0250 | 1.0250 |
| 3 | 1.0250 | 1.0250 |
| 4 | 0.9955 | 1.0017 |
| 5 | 0.9380 | 0.9545 |
| 6 | 0.9748 | 0.9794 |
| 7 | 1.0170 | 1.0173 |
| 8 | 1.0009 | 1.0015 |
| 9 | 1.0188 | 1.0198 |

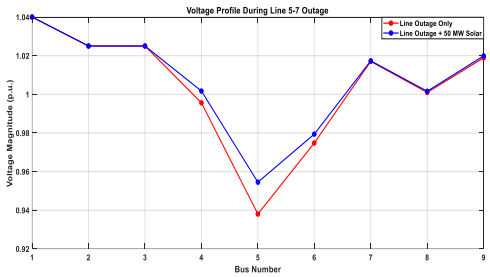


**Figure 9 Voltage Profile Comparison During Line 5-7 Outage.**

### 3.1.2. Stability Analysis During Fault Condition

**IEEE 9-Bus System Without Fault**

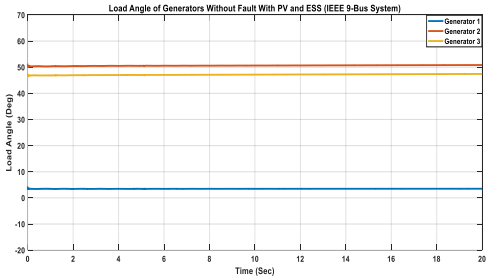


**Figure 10 Load Angle of Generators for Integrated IEEE 9-Bus System Without Fault**

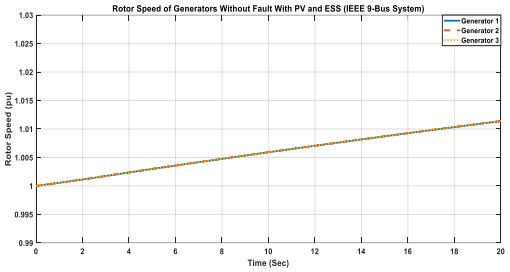


**Figure 11 Rotor Speed of Generators for Integrated IEEE 9-Bus System Without Fault**

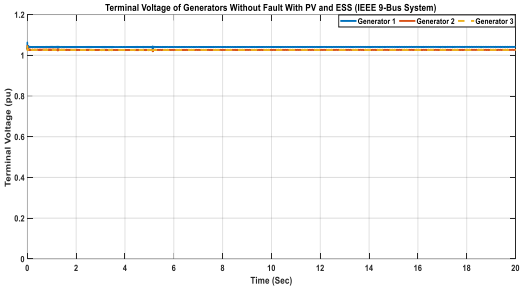


**Figure 12 Terminal Voltage of Generators for Integrated IEEE 9-Bus System Without Fault**

**IEEE 9-Bus System with Fault at Bus 1 (Generator 1 - Swing Bus)**

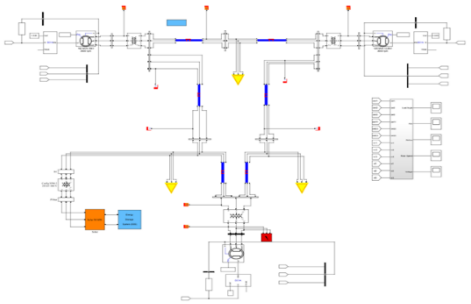

**Figure 13 IEEE 9-Bus System Model in MATLAB/Simulink with PV and ESS with Fault at Bus 1.**

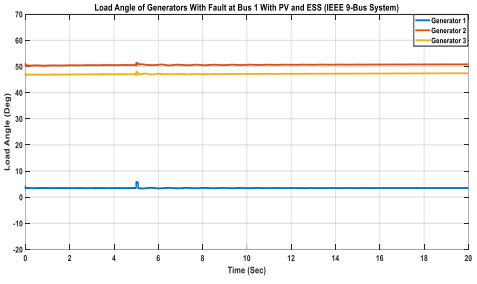


**Figure 14 Load Angle of Generators for IEEE 9-Bus System with PV and ESS with Fault at Bus 1**

International Research Journal on Advanced Engineering and Management
https://goldncloudpublications.com
https://doi.org/10.47392/IRJAEM.2026.0351
e ISSN: 2584-2854
Volume: 04 Issue: 06
June 2026
Page No: 2434 - 2443

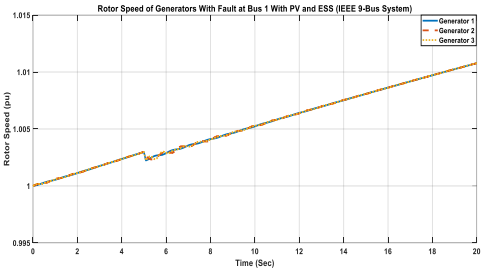


**Figure 15** Rotor Speed of Generators for IEEE 9-Bus System with PV and ESS with Fault at Bus 1

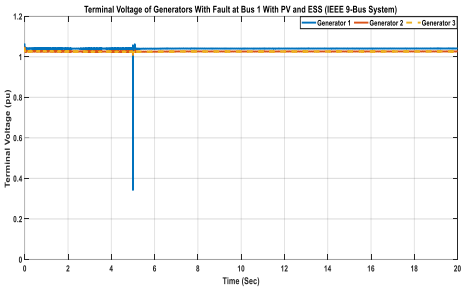


**Figure 16** Terminal Voltage of Generators for IEEE 9-Bus System with PV and ESS with Fault at Bus 1

## IEEE 9-Bus System with Fault at Bus 2 (Generator 2 - PV Bus)

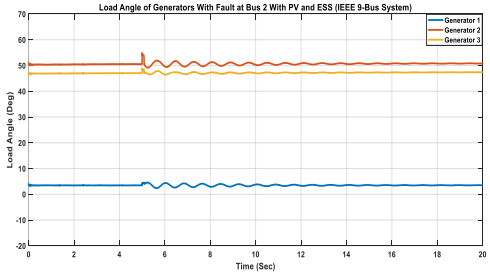


**Figure 17** Load Angle of Generators for IEEE 9-Bus System with PV and ESS with Fault at Bus 2

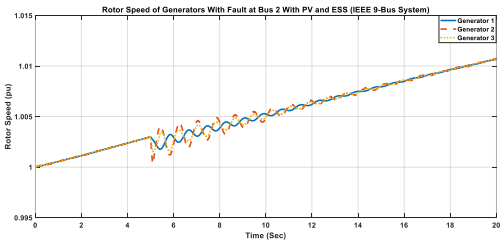


**Figure 18** Rotor Speed of Generators for IEEE 9-Bus System with PV and ESS with Fault at Bus 2

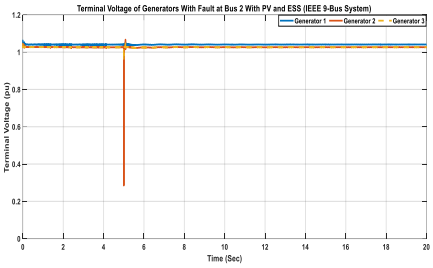


**Figure 19** Terminal Voltage of Generators for IEEE 9-Bus System with PV and ESS with Fault at Bus 2

## IEEE 9-Bus System with Fault at Bus 3 (Generator 3 - PV Bus)

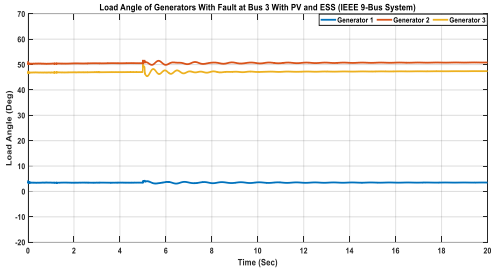


**Figure 23** Load Angle of Generators for IEEE 9-Bus System with PV and ESS with Fault at Bus 3

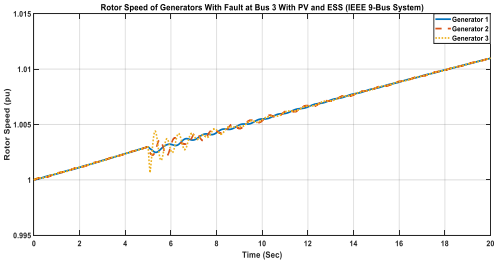


**Figure 24** Rotor Speed of Generators for IEEE 9-Bus System with PV and ESS with Fault at Bus 3

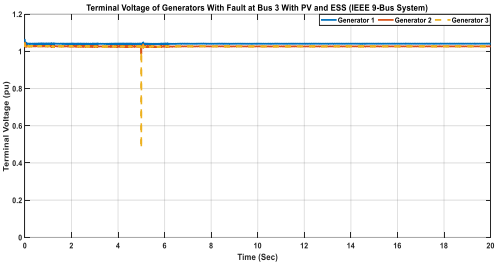


**Figure 25** Terminal Voltage of Generators for IEEE 9-Bus System with PV and ESS with Fault at Bus 3

International Research Journal on Advanced Engineering and Management
https://goldncloudpublications.com
https://doi.org/10.47392/IRJAEM.2026.0351
e ISSN: 2584-2854
Volume: 04 Issue: 06
June 2026
Page No: 2434 - 2443

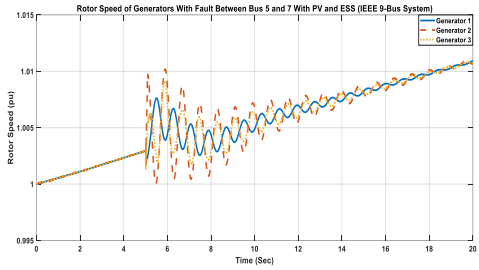


**Figure 26 Rotor Speed of Generators for IEEE 9-Bus System with PV and ESS with Fault Between Bus 5 and 7**

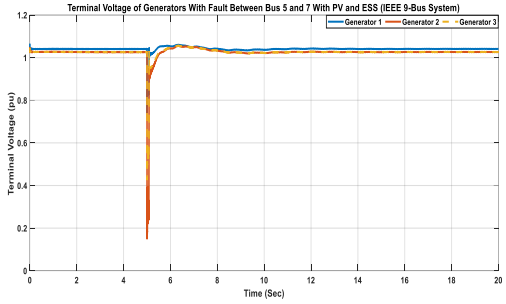


**Figure 27 Terminal Voltage of Generators for IEEE 9-Bus System with PV and ESS with Fault Between Bus 5 and 7**

The load angle response of the three synchronous generators during the three-phase-to-ground (LLLG) fault applied from 5 s to 5.08 s shows that all generators initially operate under stable steady-state conditions with nearly constant rotor angles. During fault occurrence, small transient oscillations appear due to the disturbance; however, the oscillations are well damped and settle quickly after fault clearing, indicating that generator synchronism is successfully maintained. The absence of continuously increasing rotor angle deviation confirms that the integrated PV and ESS system effectively enhances transient stability and prevents loss of synchronism under severe fault conditions. The rotor speed response during the LLLG fault at different buses and transmission lines indicates that all generators operate close to the nominal synchronous speed of 1 p.u. before the fault. Slight speed deviations and small oscillations occur during the fault due to the imbalance between mechanical input and electrical output power. However, the rotor speeds rapidly stabilize without sustained oscillations, demonstrating strong electromechanical stability. The integrated PV and ESS system effectively damps transient oscillations and supports frequency stabilization during and after the disturbance. The terminal voltage response under the LLLG fault condition shows a temporary voltage dip, especially when the fault occurs near generator buses. After fault clearance at 5.08 s, the terminal voltages recover rapidly and return to stable operating conditions without prolonged oscillations. The fast voltage recovery demonstrates the effectiveness of the integrated PV and ESS system in providing voltage support and improving fault ride-through capability, thereby enhancing the overall transient stability of the IEEE 9-bus system.

## Conclusion

This paper presented a detailed investigation on the enhancement of voltage stability and transient stability of the IEEE 9-bus power system through the coordinated integration of a 50 MW solar photovoltaic (PV) system and a 50 MWh Battery Energy Storage System (BESS). The complete analysis was carried out using MATLAB scripting and MATLAB/Simulink environments under steady-state, contingency, and fault conditions. Initially, Newton–Raphson load flow analysis confirmed that the IEEE 9-bus system operated within acceptable voltage limits with fast convergence and low transmission losses under normal operating conditions. Loss Sensitivity Factor (LSF) and Voltage Stability Index (VSI) analyses successfully identified Bus 5 as the weakest bus in the system due to its lowest voltage magnitude and highest sensitivity characteristics. Based on these results, the PV and ESS system was integrated at Bus 5 to improve overall network performance. The obtained results confirmed that the proposed renewable energy integration significantly enhanced the voltage profile of the system. The voltage at Bus 5 improved from 0.9956 p.u. to 1.0009 p.u. under normal operating conditions, while improved voltage regulation was also observed at nearby buses. Furthermore, comparative analysis showed that increasing the renewable penetration beyond 50 MW provided only marginal improvement while increasing system cost and control complexity, thereby confirming that the selected 50 MW PV and 50 MWh ESS configuration

International Research Journal on Advanced Engineering and Management
https://goldncloudpublications.com
https://doi.org/10.47392/IRJAEM.2026.0351
e ISSN: 2584-2854
Volume: 04 Issue: 06
June 2026
Page No: 2434 - 2443

is technically and economically optimal. Contingency analysis under transmission line outage conditions further verified the effectiveness of the proposed system. During the outage of the line between Bus 5 and Bus 7, the voltage at Bus 5 dropped to 0.9380 p.u. in the absence of renewable support, indicating poor voltage stability. After integrating the PV and ESS system, the voltage recovered to 0.9545 p.u., restoring the system within the acceptable operating range. Similarly, transient stability analysis under severe three-phase-to-ground (LLLG) fault conditions demonstrated that the integrated PV and ESS system effectively reduced rotor oscillations, improved damping performance, maintained generator synchronism, and provided rapid voltage recovery after fault clearance. Therefore, the obtained results confirm that the coordinated integration of a properly sized solar PV plant and Battery Energy Storage System at an optimally selected weak bus effectively improves voltage stability, transient stability, fault ride-through capability, frequency support, and overall operational reliability of the IEEE 9-bus power system. The developed methodology and simulation framework can be effectively utilized for future renewable-integrated smart grid and power system stability studies.

## References

[1]. REN21, "Renewables 2023 Global Status Report," 2023.
[2]. International Energy Agency (IEA), "World Energy Outlook 2023," 2023.
[3]. P. Kundur et al., "Definition and classification of power system stability," IEEE Trans. Power Systems, vol. 19, no. 2, pp. 1387–1401, 2004.
[4]. J. Machowski et al., Power System Dynamics: Stability and Control, Wiley, 2008.
[5]. M. Ulbig, T. Borsche, and G. Andersson, "Impact of low rotational inertia on power system stability," IEEE Trans. Power Systems, vol. 29, no. 2, pp. 1–9, 2014.
[6]. Y. Zhang et al., "Review on frequency stability of power systems with high renewable penetration," Renewable and Sustainable Energy Reviews, vol. 81, pp. 1–13, 2020.
[7]. Molina-García et al., "Stochastic optimization for renewable energy systems," IEEE Trans. Power Systems, vol. 32, no. 2, pp. 1–10, 2021.
[8]. X. Luo et al., "Overview of energy storage technologies," Applied Energy, vol. 137, pp. 511–536, 2015.
[9]. H. Bevrani, et al., "Power system frequency control with energy storage systems," IEEE Trans. Smart Grid, vol. 10, no. 1, pp. 1–10, 2019.
[10]. S. Teleke et al., "Control strategies for battery energy storage," IEEE Trans. Energy Conversion, vol. 25, no. 3, pp. 1–10, 2020.
[11]. H. Yang et al., "Optimal sizing of hybrid renewable systems," Solar Energy, vol. 81, pp. 76–84, 2007.
[12]. J. Guerrero et al., "Hierarchical control of microgrids," IEEE Trans. Industrial Electronics, vol. 58, no. 1, pp. 158–172, 2011.
[13]. M. Shahidehpour, et al., "Smart grid control strategies," IEEE Trans. Smart Grid, vol. 12, no. 1, pp. 1–10, 2021.
[14]. MathWorks, "Renewable Energy Systems Simulation Using MATLAB/Simulink," 2024.
[15]. J. Carpentier, "Optimal power flow," Electric Power Systems Research, vol. 1, pp. 3–15, 1962.